WARSAW UNIVERSITY OF TECHNOLOGY Index 351733
FACULTY OF CIVIL ENGINEERING
COMMITTEE FOR CIVIL AND WATER ENGINEERING
POLISH ACADEMY OF SCIENCES ISSN 1230-2945

DOI: 10.24425/ace.2026.158625

ARCHIVES OF CIVIL ENGINEERING

Vol. LXXII ISSUE 2 2026

 pp. 529 – 544

Research paper

Optimizing of concreting method in mass concrete structure using numerical analysis (roller compacted concrete gravity dam)

Theo Alfaro Dida Darmajaya[1], Bambang Supriyadi[2], Suprapto Siswosukarto[3]

Abstract: In mass concrete structures, the increase in temperature due to hydration heat must be carefully studied to minimize the risk of thermal cracking. Gravity dams, a type of mass concrete structure, rely on their own weight to resist the pressure of water. An important innovation in civil construction is Roller-Compacted Concrete (RCC), a form of concrete compacted using a roller compactor. In this study, 3D numerical simulations were conducted using Midas Civil software to analyze the development of hydration temperature within the RCC Tannur Gravity Dam structure in Jordan. The 3D geometric modeling was limited to the cross-section (middle section) of a 15-meter-wide monolithic dam block, assuming symmetry on both sides of the section. Adiabatic boundary conditions were applied to the model to prevent heat loss from the cement hydration reaction. A construction stage analysis was conducted to determine the temperature evolution during each stage of concrete placement. Several simulation scenarios were analyzed, varying the layer thickness (3 m and 4 m), the concreting sequence, and the initial placement temperature of the RCC (20°C, 25°C, 30, and 35°C). Concreting Scheme 2 not only lowers the maximum hydration heat temperature and the associated thermal stress but also speeds up the construction of a dam block by increasing the RCC layer thickness. The results of the numerical modeling demonstrated that controlling the heat of hydration in mass concrete structures can be effectively achieved by optimizing construction methods and parameters.

Keywords: gravity dam, heat of hydration, mass concrete, midas civil, roller compacted concrete

[1]Student, Gadjah Mada University, Department of Civil and Enviromental Engineering, Sleman, Daerah Istimewa Yogyakarta, Indonesia, e-mail: theoalfarodidadarmajaya@mail.ugm.ac.id, ORCID: 0009-0001-1197-9520
[2]Prof., Ir., CES., DEA., PhD., IPU., ASEAN. Eng., Gadjah Mada University, Department of Civil and Enviromental Engineering, Sleman, Daerah Istimewa Yogyakarta, Indonesia, e-mail: bambang.supri@ugm.ac.id, ORCID: 0009-0008-1124-4015
[3]Ir., PhD., IPM., Gadjah Mada University, Department of Civil and Enviromental Engineering, Sleman, Daerah Istimewa Yogyakarta, Indonesia, e-mail: suprapto.siswosukarto@ugm.ac.id, ORCID: 0009-0007-8976-4275

1. Introduction

Dams can be constructed in various shapes and using different methods to meet specific needs and functions [1]. A gravity dam is a type of dam that resists water pressure using its own weight [2]. These dams are often built with concrete, a fundamental material in civil engineering construction. An innovative approach in civil engineering is the use of Roller-Compacted Concrete (RCC). RCC is essentially concrete that is compacted using a roller compactor [3]. Since dam construction requires an enormous quantity of concrete, it falls under the category of mass concrete structures. In such structures, it is crucial to monitor the temperature increase caused by the cement hydration reaction to minimize the risk of thermal cracking [4]. The use of numerical simulation software to model hydration heat makes it easier to evaluate temperature rises and thermal stresses in mass concrete structures, ensuring better design and construction practices.

Many previous research devoted to evaluate the heat of hydration in mass concrete structures using finite element software. Malkawi et al. [5] used ANSYS software with 2D and 3D finite element methods to analyze the heat generated from cement hydration in the Tannur Dam. Their construction stage analysis demonstrated the temperature and stress distribution in the concrete at each stage. A three-dimensional analysis using Midas Civil software was conducted by Van-Lam et al. [6] to determine the maximum temperature of hydration heat, which depends on the thickness of the concrete layers and the initial temperature of the RCC. While increasing the layer thickness can accelerate the construction process, it also raises the risk of thermal cracking due to the heat of hydration, potentially affecting the durability of the concrete [7]. Key factors such as initial temperature, modulus of elasticity, tensile stress capacity, concreting schedule, number of layers, and concrete layer thickness must be carefully considered in the numerical analysis of hydration heat [8].

Based on previous research, numerical modeling has proven to be a powerful tool for predicting the development of cement hydration heat in dam structures. The temperature increase caused by hydration heat in mass concrete structures is significantly influenced by factors such as thermal properties, environmental conditions, initial concrete temperature, and concrete casting methods [9, 10]. This study extends the temperature analysis of hydration heat in the Tannur Dam, Jordan, previously conducted by Malkawi et al. [5] and Pravathi et al. [7]. It specifically examines the effects of layer thickness, concreting schemes, and the initial temperature of the concrete during placement on the percentage increase in temperature caused by hydration heat. Unlike the earlier studies that utilized ANSYS software, this research employs Midas Civil software for finite element method (FEM) analysis to provide additional insights into the thermal behavior of the dam structure.

2. Methodology

2.1. Tannur gravity dam

The object studied is the Tannur Dam with a height of 56 m and a length of 242 m in Jordan, Middle East. The Tannur Dam was built using Roller Compacted Concrete (RCC), which made in layers with 300 mm thickness and the upstream face of the dam composed of Grout Enriched Roller Compacted Concrete (GE-RCC) [7]. The dimensions of the dam 3D model are presented in Fig. 1.

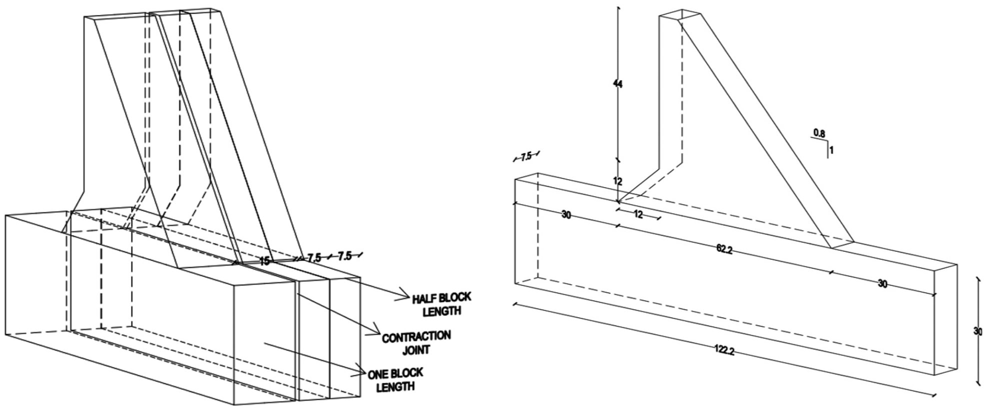

(a) (b)

Fig. 1. Tannur Dam 3D geometry: (a) section cut; (b) half block length (dimensions in meter)

2.2. Research procedures

As part of the research planning and to simplify the research process, the research steps were arranged in the form of a flow chart as shown in Fig. 2.

The Tannur Dam was constructed using 12 RCC blocks, each approximately 15 meters long [7]. The concrete was placed in 19 layers over 10 days per layer, with a thickness of 3 meters for each layer, except for the final layer, which was 2 meters thick. The thermal and structural properties of RCC concrete used for hydration heat analysis are presented in Tables 1 and 2, while the adiabatic temperature rise for Jordanian cement is shown in Fig. 3. The Tannur Dam was built in 12 blocks so that each had a length of 20 m. However according to the design report by Howard Humpreys [11], the actual size of the constructed block was about 15 m [5]. Thus, in this this research the 3D geometry of the dam is based on research by Malkawi et al. [5]. Numerical analysis of initial condition which is a layer thickness of 3 m and concrete initial temperature of 20°C must be carried out first to check the validity of the analysis results by comparing the results obtained with previous research by Malkawi et al. [5] and Parvathi et al. [7].

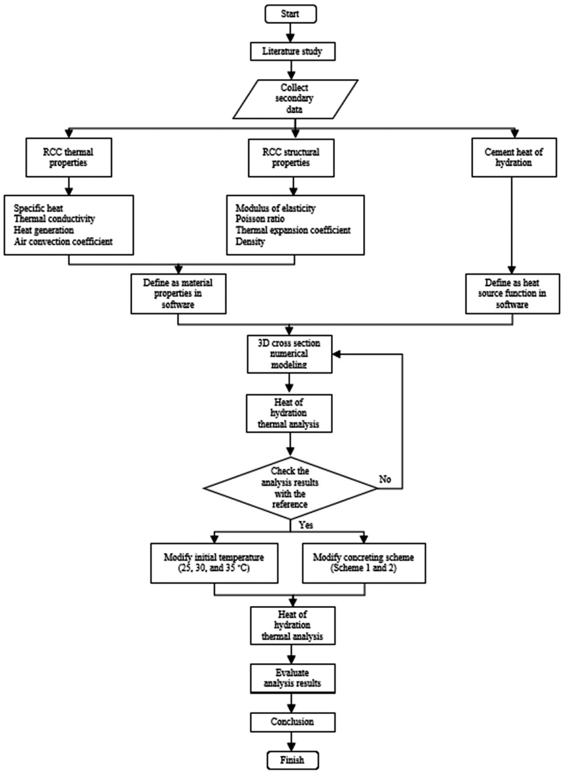

Fig. 2. Research flow chart

2.3. Data for numerical analysis

The data utilized in this research consists of secondary information obtained from a previous study carried out by Malkawi et al. [5] and Parvathi et al. [7], as shown in Table 1 and Table 2. The concrete mix consisted of 125 kg/m^3 of cement and 75 kg/m^3 of pozzolan (Class N fly ash) [12]. According to the Jordanian Ordinary Portland Cement (OPC) test results, the heat of hydration of the concrete at 28 days was 309 J/g [5]. The compressive strength of the concrete at 28 days was 16.7 MPa, increasing to 19.8 MPa at 90 days [12].

Table 1. RCC thermal properties [5, 7]

Number	Properties	Value
1	Specific heat	963 J/(kg·°C)
2	Thermal conductivity	2,6 J/(m·s·°C)
3	Heat generation at 28 days	309 J/g
4	Air convection coefficient	15 J/(s·m2)

Table 2. RCC structural properties [5,7]

Number	Properties	Value
1	Concrete modulus of elasticity	18 GPa
2	Poisson ratio	0,2
3	Thermal expansion coefficient	6,5×106 /°C
4	Density	2.400 kg/m3

The hydration heat of Jordanian cement in this study is defined as heat source function in the Midas Civil software with the value presented in Fig. 3.

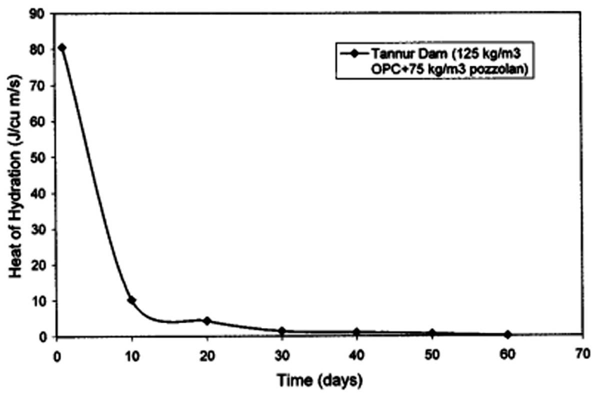

Fig. 3. Cement heat of hydration as heat source function [5]

The data used to compare the results of the present study with previous research carried out by Malkawi et al. [5] and Parvathi et al. [7], as well as to validate the numerical modeling, includes temperature measurements from thermocouples and the maximum hydration heat temperature for a layer thickness of 3 meters as shown in Table 3.

Table 3. Heat of hydration temperature reference for a layer thickness of 3 m

Number	Number of Spreading Layer	Maximum Temperature (°C)		
		Malkawi et al. [5]	**Thermocouple [5]**	**Parvathi et al. [7]**
1	3rd	36.49	34	34.66
2	6th	37.39	38	37.90
3	12th	37.79	38	37.70
4	19th	37.75	37	36.75

2.4. Analysis method

The heat transfer analysis of the Tannur Dam's RCC structure was conducted using Midas Civil software. Before initiating numerical modelling, the following conditions were established:

a) 3D Geometric Modelling: The analysis focused solely on the cross-section (middle section) of the 15-meter monolithic dam block, assuming symmetry on both sides of the dam section [13, 14].
b) Ambient Temperature: A constant ambient temperature of 12°C was assumed throughout the construction process [5, 7].
c) Foundation Conditions: The dam foundation was modelled as rock with a constant temperature of 18°C [5, 7].
d) Air Convection: The air convection coefficient was applied only to the surfaces of the dam exposed to the ambient temperature.
e) Adiabatic Condition: This assumption is based on [15] and [16], considering mass concrete structure.
f) Applied Load: The only load considered in the analysis was the self-weight of the dam.

There is a potential for thermal cracking in the mass concrete structures. Therefore, during the conreting process it is necessary to impose limitations by creating concrete blocks to prevent temperature buildup from causing thermal cracking. This study simulates the approach for optimizing block sizes and concreting schemes.

The heat diffusion equation shown in Equation (2.1) [17, 18]:

$$\lambda\left(\frac{\partial^2 T}{\partial x^2}+\frac{\partial^2 T}{\partial y^2}+\frac{\partial^2 T}{\partial z^2}\right)+Q_h=\rho\cdot C_p\cdot\frac{\partial T}{\partial t} \tag{2.1}$$

where: Q_h – rate of heat generation per unit volume, ρ – density of concrete (kg/m^3), C_p – specific heat (J/(kg·°C)), λ – thermal conductivity (J/(m·h·°C)), T – temperature (°C), t – time (h).

The heat generated from cement hydration was evaluated by the following Equation (2.2), proposed by Tanabe et al. [19, 20].

$$Q(t)=Q_\infty(1-e^{-\alpha t}) \tag{2.2}$$

where: $Q(t)$ – heat generated as function of time (°C), Q_∞ – maximum adiabatic temperature rise (°C), α – coefficient of the temperature rise, t – time (days).

For adiabatic condition, the value of $\lambda = 0$. If Equation (2.1) and (2.2) is combined, Equation (2.3) can be obtained as follows [21].

$$Q_h=\rho C_p Q_\infty \alpha e^{-\alpha t} \tag{2.3}$$

According to Tatro and Schrader [22] in Malkawi et al. [5], the strain that arises can be calculated using Equation (2.4).

$$\text{induced strain}=(C_{\text{th}})(\mathrm{d}T)(K_R)(K_f) \tag{2.4}$$

where: C_{th} – thermal expansion coefficient, dT – temperature change, K_R – structural restraint factor, K_f – foundation restrain factor.

2.5. Three-dimension numerical modeling

The Midas Civil software was employed to analyse temperature variations in concrete caused by hydration heat. The dam was modelled from the foundation (subsoil) to the main concrete structure using four-node solid elements, as illustrated in Fig. 4. Solid elements are made using plate elements for the subsoil section and concrete structures which are extruded 7.5 m, thus representing half of the concrete block. Since the model created is a $\frac{1}{2}$ symmetrical model, boundary conditions are set to restrain translational DOFs to each axis because solid elements do not restrain rotational DOFs [23]. Ambient temperature and convection coefficient are determined on the part of the dam that is exposed to the atmosphere, namely the outer surface of the dam and the joint surface between concrete castings.

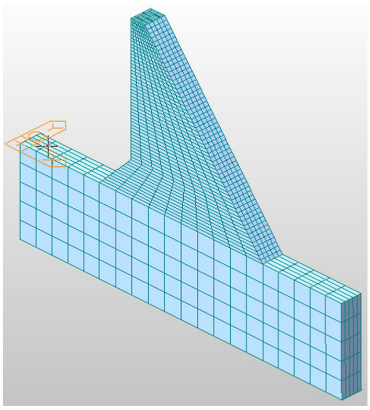

Fig. 4. Tannur Dam 3D model

The concrete placement process for the Tannur RCC dam construction required 10 days (240 hours) per layer [7]. In the construction stage analysis in Midas Civil Software, the time interval for each layer placement was divided into increments of 24, 48, 72, 96, 144, 168, 192, 216, and 240 hours. These time intervals were applied to each construction stage, resulting in a cumulative timeline at the conclusion of the construction process.

As an initial step, a hydration heat analysis was performed for a 3-meter layer thickness, based on project reports used for modelling validation. After confirming that the analysis results were accurate, the study progressed by modifying key parameters, including layer thickness, concreting schemes, and the initial concrete temperature. The primary difference between Concreting Scheme 1 and Concreting Scheme 2 lies in the division of each concrete block layer into two parts, as illustrated in Fig. 5. For a 3-meter layer thickness, the spreading thickness was assumed to be 0.3 meters in Scheme 1 and 0.6 meters in Scheme 2. Similarly, for a 4-meter layer thickness, the spreading thickness was set at 0.4 meters for Scheme 1 and 0.8 meters for Scheme 2. The initial temperature of the concrete, based on the studies by Malkawi et al. [5] and Parvathi et al. [7], was set at 20°C. To evaluate the impact of initial concrete temperature on hydration heat, this temperature was varied to 25°C, 30°C, and 35°C in the analysis for hot weather concreting [24].

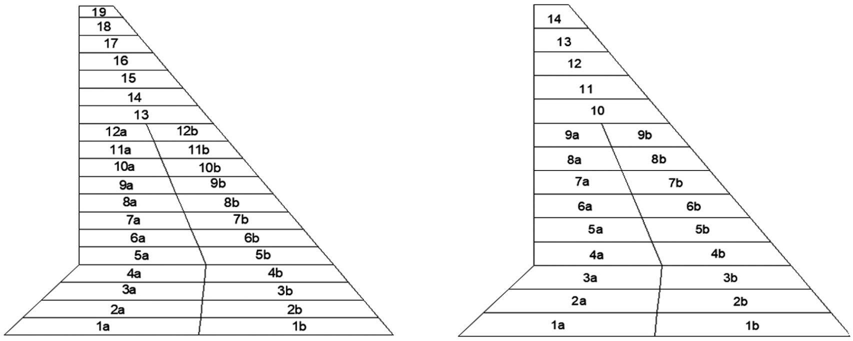

(a) (b)

Fig. 5. Concreting scheme 2: (a) 3 m thickness; (b) 4 m thickness

3. Results and discussion

3.1. Validation of the numerical model

The results of the hydration heat simulation for a 3-meter concrete layer thickness are presented in Table 4. Overall, when compared with previous research, the results exhibit an error percentage of less than 2%. This confirms that the modeling method employed in this study is accurate and reliable.

Table 4. Heat of hydration temperature reference for a layer thickness of 3 m

Number	Number of Spreading Layer	Maximum Temperature (°C)	Error Percentage		
			Malkawi et al. [5] (%)	Thermocouple [5] (%)	Parvathi et al. [7] (%)
1	3^{rd}	34.13	6.47	0.38	1.53
2	6^{th}	37.20	0.51	2.11	1.85
3	12^{th}	38.00	0.56	0.00	0.80
4	19^{th}	37.44	0.82	1.19	1.88

3.2. Increase in layer thickness, concreting scheme, and concrete initial temperature

Increasing the casting layer thickness can reduce construction time, but it also affects the rise in hydration heat temperature. In this study, concreting was modeled for a 4-meter layer thickness, assuming each layer was worked on for 10 days, with a total of 14 layers. At the end of the concreting process, the temperature increased by 2.15°C compared to the 3-meter thickness. As shown in Fig. 6, the temperature distribution reveals the highest temperature at the center zone, with the temperature history shown in Fig. 7. A decrease in temperature was observed in both layer thicknesses before it rose again. This fluctuation occurred due to the casting of subsequent layers, which caused the temperature of the previously cooled concrete to rise again. The percentage increase in temperature for each spreading layer of 3-meter and 4-meter thicknesses is presented in Table 5. The greatest increase occurred after three layers of concrete were spread, with a rise of 2.72%. This temperature rise was primarily caused by the heat trapped within the concrete layers, which made it more difficult for the heat to dissipate in the 4-meter-thick layers.

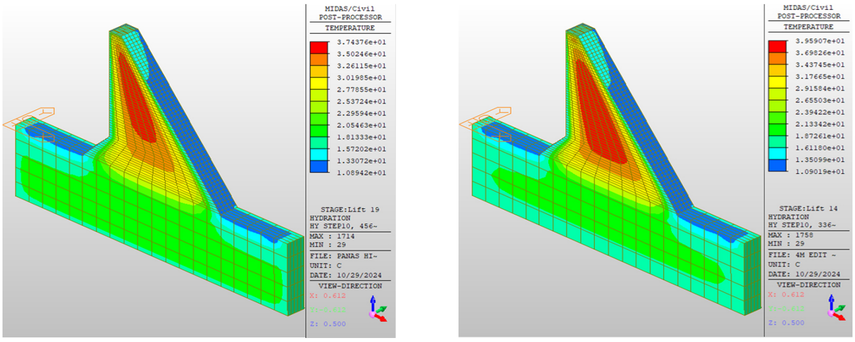

(a) (b)

Fig. 6. Temperature contour at the end of concreting scheme 1: (a) 3 m thickness; (b) 4 m thickness

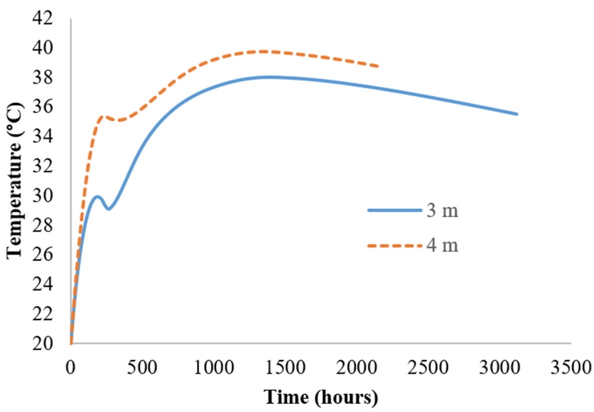

Fig. 7. Temperature history concreting scheme 1 at the center of the dam

Table 5. Percentage increase in temperature 3 m to 4 m layer thickness

Number	**Number of Spreading Layer**	**Maximum Temperature (°C)**		**Percentage Increase (%)**
		3 m Thickness	**4 m Thickness**	
1	3rd	34.13	36.85	2.72
2	6th	37.20	39.31	2.11
3	9th	37.97	39.75	1.78
4	12th	38.00	39.73	1.73
5	Last	37.44	39.59	2.15

The concreting method significantly influences the development of hydration heat in concrete dam construction. In this study, modeling was conducted by dividing each spreading layer into two parts, as illustrated in Fig. 5. The temperature contour in Fig. 8 shows that, at the end of the concreting period in Scheme 2, the temperature at the center of the dam has decreased. This is further highlighted in Fig. 9, where the maximum temperature reduction for layer thicknesses of 3 meters and 4 meters is 1.94% and 2.10%, respectively.

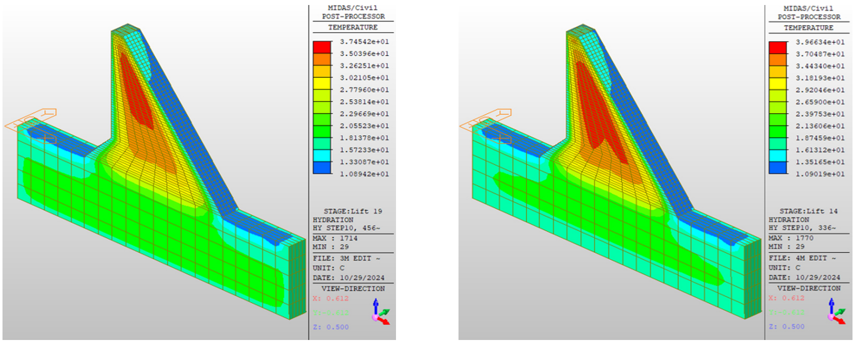

(a) (b)

Fig. 8. Temperature contour at the end of concreting scheme 2: (a) 3 m thickness; (b) 4 m thickness

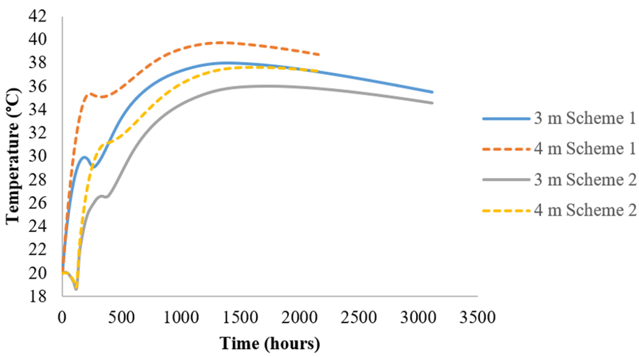

Fig. 9. Comparison graph of the increase in hydration heat temperature between schemes

The maximum temperature of hydration heat increases significantly with higher initial concrete temperatures. The highest maximum concrete temperature is observed at an initial temperature of 35°C, followed by 30°C, 25°C, and 20°C for each scheme. As shown in Fig. 10 and Fig. 11, in Scheme 2, the temperature decreases to approximately 20°C within the first 120 hours of concreting for each layer thickness and initial concrete temperature. The higher the initial concrete temperature, the greater the temperature drop during this period. This decrease is due to convection between the concrete and the ambient temperature at the point under consideration. Once concreting continues for part b (the right side), the temperature begins to rise again, eventually reaching its maximum value.

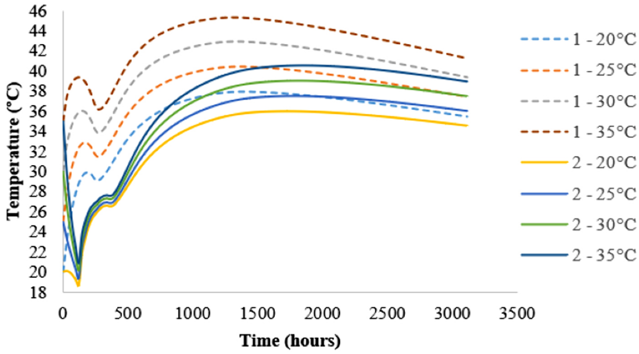

Fig. 10. Hydration heat temperature for a layer thickness of 3 m with variations in the initial temperature of the concrete

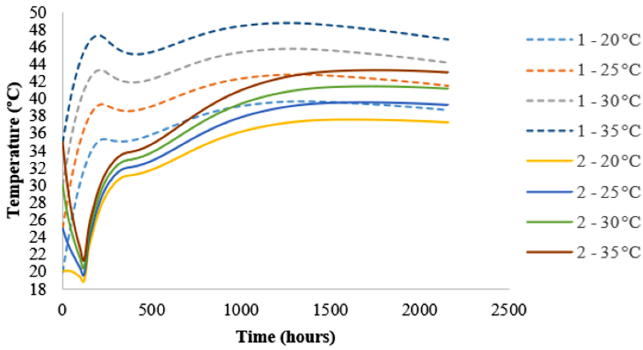

Fig. 11. Hydration heat temperature for a layer thickness of 4 m with variations in the initial temperature of the concrete

3.3. Stress-strain control and crack width estimation

The induced strain is calculated using Equation (2.4), assuming $K_R = K_F = 1$ to obtain more conservative results. The minimum temperature used in the calculations is 12°C, consistent with the ambient temperature assumption in the numerical analysis. The tensile strain capacity value of 80 μm/m was derived from Dunstan's [25] research as cited by [5]. Based on the calculation results in Table 6, the induced strain exceeds the tensile strain capacity of the concrete, indicating the necessity of contraction joints to minimize cracking. The smallest tensile strain values for 3-meter and 4-meter layer thicknesses were observed in Scheme 2 concreting with an initial temperature of 20°C. Furthermore, the tensile strain values for 4-meter thickness in Scheme 2 at all initial temperatures are consistently lower than those for 3-meter thickness in Scheme 1. These findings confirm that Scheme 2, which involves dividing each layer into two concrete blocks, effectively reduces both the maximum hydration heat temperature and the induced strain values.

Table 6. Tensile strain and crack width estimation

Thickness (m)	Scheme	Initial Temperature (°C)	Maximum Temperature (°C)	ΔT (°C)	Induced Strain (μmm)	Excess Strain (μmm)	Crack Width Estimation (mm)
3	1	20	37.99	25.99	168.91	88.91	21.52
		25	40.44	28.44	184.84	104.84	25.37
		30	42.89	30.89	200.80	120.80	29.23
		35	45.36	33.36	216.81	136.81	33.11
	2	20	36.04	24.04	156.29	76.29	18.46
		25	37.54	25.54	166.02	86.02	20.82
		30	39.04	27.04	175.79	95.79	23.18
		35	40.55	28.55	185.59	105.59	25.55
4	1	20	39.72	27.72	180.21	100.21	24.25
		25	42.73	30.73	199.74	119.74	28.98
		30	45.74	33.74	219.32	139.32	33.71
		35	48.76	36.76	238.95	158.95	38.47
	2	20	37.62	25.62	166.53	86.53	20.94
		25	39.51	27.51	178.84	98.84	23.92
		30	41.42	29.42	191.22	111.22	26.91
		35	43.33	31.33	203.63	123.63	29.92

The occurrence of strain in the concrete indicates that the structure is experiencing tensile stress due to the accumulation of hydration heat. Based on the estimated crack width calculations, it can be concluded that the dam structure has the potential for thermal cracking under all conditions. Therefore, the concreting process for the Tannur Dam needs to be divided into concrete blocks to minimize thermal cracking, with an allowable crack width assumed to be 2.5 mm [5]. The actual size of the constructed block was about 15 m, while the total width of the dam is 242 m [5]. The calculation of the minimum block width to control thermal stress is presented in Table 7.

Based on the calculations in Table 7, it is evident that increasing the initial concreting temperature affects the minimum number of required concrete blocks. There are several measures that can be implemented to decrease the temperature of concrete, such as using admixtures, ice addition, and liquid nitrogen injection [24]. Concreting scheme 2 is effective in reducing the minimum number of required concrete blocks. The minimum number of concrete blocks required for Scheme 2 with a thickness of 4 m is less than that for Scheme 1 with a thickness of 3 m. Therefore, Concreting Scheme 2 can accelerate the required construction process.

Table 7. Minimum block width to control stress

Thickness (m)	Scheme	Initial Temperature (°C)	Crack Width Estimation (mm)	Minimum Number of Blocks	Minimum Block Width (m)
3	1	20	21.52	9	27
		25	25.37	11	22
		30	29.23	12	20
		35	33.11	14	17
	2	20	18.46	8	30
		25	20.82	9	27
		30	23.18	10	24
		35	25.55	11	22
4	1	20	24.25	10	24
		25	28.98	12	20
		30	33.71	14	17
		35	38.47	16	15
	2	20	20.94	9	27
		25	23.92	10	24
		30	26.91	11	22
		35	29.92	12	20

3.4. Construction cost estimation

In dam construction, cost and construction time are critical factors to consider. The Willow Creek Dam, standing 52 meters high, with a total of 330.000 m^3 RCC was placed in less than five months, with an average in-place cost of approximately 26 per m^3 [26]. The time required to complete one layer of RCC (Roller Compacted Concrete) for the Tannur Dam with a thickness of 3 m and 4 m is 10 days [7]. The width of one block of the Tannur Dam modeled in this study is 15 m, with a total volume of 24,432 m^3 of RCC. The cost to construct one block with a width of 15 m is 635,232, assuming an RCC concreting cost of 26 per m^3 [26]. The modeled Tannur Dam has a height of 56 m. If a layer thickness of 3 m is used, 19 layers are required, with a total construction time of 190 days. Meanwhile, for a layer thickness of 4 m, 14 layers are needed, with a total construction time of 140 days. Based on the calculations in Tables 6 and 7, the concreting of RCC with a thickness of 4 m can be implemented using concreting Scheme 2, reducing the construction time for one dam block to 140 days. It can be concluded that concreting Scheme 2 not only reduces the maximum hydration heat temperature and resulting thermal stress but also accelerates the construction process for one dam block by increasing the thickness of the RCC layers.

4. Conclusions

The heat of hydration in mass concrete structures is a critical factor to control, as it significantly influences the selection of material types and construction methods. A reduced water content in RCC can effectively lower the temperature rise caused by hydration heat. Numerical modeling shows that the thickness of the concrete layer, both in the vertical and horizontal directions, directly affects the temperature distribution, particularly at the center of the dam.

The key conclusions derived from this research are as follows:

a. Maximum Temperature and Initial Concrete Temperature:

- The highest temperatures from hydration heat were recorded in Scheme 1 with layer thicknesses of 3 m and 4 m at an initial concreting temperature of 35°C, reaching 45.36°C and 48.76°C, respectively.
- Increasing the initial concreting temperature from 20°C to 35°C results in a rise in maximum hydration temperature of up to 7.37% for the 3 m layer thickness and 9.04% for the 4 m layer thickness.
- To mitigate this temperature increase, incorporating cold water in the concrete mix design is recommended to reduce the initial temperature of the concrete.

b. Effectiveness of Concreting Scheme 2:

- Scheme 2 reduces the maximum hydration temperature for layer thicknesses of 3 m and 4 m by:
- 1.94% and 2.10% at an initial temperature of 20°C,
- 2.89% and 3.21% at an initial temperature of 25°C,
- 3.85% and 4.32% at an initial temperature of 30°C.
- 4.8% and 5.43% at an initial temperature of 35°C.
- In Scheme 2, the concrete temperature at the middle of the dam decreases significantly during the first 120 hours of concreting due to convection with the ambient temperature. This occurs before concreting continues for the next section, contributing to temperature reduction.

c. Tensile Strain and Temperature Difference (ΔT):

- The difference between the maximum hydration temperature of the concrete and the ambient temperature (ΔT) generates tensile strains. The greater the ΔT, the higher the tensile strain in the concrete.
- According to the calculations, the largest tensile strain occurs in Scheme 1 with a 4 m layer thickness and an initial temperature of 35°C, while the smallest tensile strain is observed in Scheme 2 with a 3 m layer thickness and an initial temperature of 20°C.
- Interestingly, for all initial temperatures, the tensile strain values in Scheme 1 with a 3 m layer thickness are still higher than those in Scheme 2 with a 4 m layer thickness.

- This highlights the importance of adjusting the concreting method during construction project. If the vertical layer thickness is increased, the horizontal layer thickness should be reduced to minimize tensile strains and mitigate potential cracking.

d. Construction Cost Estimation:

- The construction cost for a single 15 m-wide block is estimated at 635,232, based on an RCC concreting rate of 26 per cubic meter.
- By increasing the thickness of the RCC layers to 4 m, concreting Scheme 2 can accelerates the construction process for a dam block 50 days earlier.

References

[1] C. Zhang, H. Wang, J. Cao, Q. Liu, F. Liu, and M. Wang, "Type Selection between Arch Dam and Gravity Dam Based on Construction Simulation: A Case Study", *Water*, vol. 15, no. 8, art. no. 1482, 2023, doi: 10.3390/w15081482.

[2] C.F. Corns, G.S. Tarbox, and E.K. Schrader, "Gravity Dam Design and Analysis", in *Advanced Dam Engineering for Design, Construction, and Rehabilitation*, R.B. Jansen, Ed. Boston: Springer, 1988, pp. 466–492, doi: 10.1007/978-1-4613-0857-7_16.

[3] D. Rambabu, A.K. Sharma, and M.A. Akbar, "Evaluation Of Roller Compacted Concrete for Its Application as High Traffic Resisting Pavements with Fatigue Analysis", *Construction and Building Materials*, vol. 401, art. no. 132977, 2023, doi: 10.1016/j.conbuildmat.2023.132977.

[4] Y. Lyu, Y. Liu, J. Liu, and Z. Ma, "Research on Hydration-caused Thermal Cracking Risk of Steel-concrete Composite Bridge Pylons", *Journal of Constructional Steel Research*, vol. 211, art. no. 108165, 2023, doi: 10.1016/j.jcsr.2023.108165.

[5] A.I.H. Malkawi, S.A. Mutasher, and T.J. Qiu, "Thermal-Structural Modelling and Temperature Control of Roller Compacted Concrete Gravity Dam", *Journal of Performance of Constructed Facilities*, vol. 17, no. 4, pp. 177–187, 2003, doi: 10.1061/(ASCE)0887-3828(2003)17:4(177).

[6] V.L. Tang, T.C. Nguyen, B.I. Bulgakov, N.A. Pham, and T.P. Huynh, "A Combined Experiment-Simulation Study on Temperature Regime of Roll-Compacted Concrete Applying for Dam Construction", *Journal of Thermal Engineering*, vol. 6, no. 5, pp. 772–785, 2020, doi: 10.18186/thermal.799443.

[7] I.S. Parvathi and S. Shehanaz, "Thermal Transient Stress Analysis in RCC Dam Construction", *Materials Today: Proceedings,* 2023, doi: 10.1016/j.matpr.2023.02.329.

[8] A.I.H. Malkawi, D.A.H. Malkawi, and K.A. Bani-Hani, "Thermal-Structural Modelling and Temperature Control of Roller-Compacted Concrete Gravity Dam: A Parametric Study", in *4th International Conference "Coordinating Engineering for Sustainibility and Resilience" & Midterm Conference of CircularB "Implementation of Circular Economy in the Built Environment". CESARE 2024,* V. Ungureanu, L. Braganca, C. Baniotopoulos, and K.M. Abdalla, Eds. Cham: Springer, 2024, pp. 82–91, doi: 10.1007/978-3-031-57800-7_7.

[9] Y. Zhang, S. Wang, S. He, and X. Hao, "Analysis of Factors Influencing The Temperature Field Variation in Mass Concrete During Hydration Heat Release", *Case Studies in Thermal Engineering*, vol. 52, art. no. 103737, 2023, doi: 10.1016/j.csite.2023.103737.

[10] Y. Zhao, G. Li, C. Fan, W. Pang, and Y. Wang, "Effect of Thermal Parameters on Hydration Heat Temperature and Thermal Stress of Mass Concrete", *Advances in Materials Science and Engineering*, vol. 2021, art. no. 5541181, 2021, doi: 10.1155/2021/5541181.

[11] Howard Humphreys Consulting Engineers, *The Study and Design of Tannur Dam, Report,* vol. 3, 1995.

[12] S. Serdar, "State of The Art in Roller Compacted Concrete (RCC) Dams: Design and Construction", M.Sc. thesis, Middle East Technical University, Ankara, 2014.

[13] U. Mirkovic, V. Kuzmanovic, and G. Todorovic, “Long-Term Thermal Stress Analysis and Optimization of Contraction Joint Distance of Concrete Gravity Dams”, *Applied Science*, vol. 12, no. 16, art. no. 8163, 2022, doi: 10.3390/app12168163.

[14] E.Y. Sayed-Ahmed, A.A. Abdelrahman, and R.A. Embaby, “Concrete Dams: Thermal-stress and Construction Stage Analysis”, *Dams and Reservoirs*, vol. 28, no. 1, pp. 12–30, 2018, doi: 10.1680/jdare.16.00055.

[15] R.S. Foumani, A. Mardookhpour, and F. Saberi, “Optimization of Time and Temperature of Dam Construction for Thermal Analysis of Roller-compacted Concrete Dam”, *Numerical Methods in Civil Engineering*, vol. 7, no. 4, pp. 1–11, 2023, doi: 10.52547/NMCE.2022.599.1.

[16] E. Castilho, N. Schclar, C. Tiago, and M.L.B. Farinha, “FEA Model for The Hydration Process and Temperature Evolution During The Concreting of an Arch Dam”, *Engineering Structures*, vol. 174, pp. 165–177, 2018, doi: 10.1016/j.engstruct.2018.07.065.

[17] F.P. Incropera, D.P. Dewitt, T.L. Bergman, and A.S. Lavine, *Fundamentals of Mass and Heat Transfer,* 6th ed. New York: John Wiley and Sons, 2006.

[18] A. Helowicz, “Measurement and Modelling of The Temperature Distribution Caused by The Heat of Cement Hydration”, *Archives of Civil Engineering*, vol. 70, no. 3, pp. 225–239, 2024, doi: 10.24425/ace.2024.150980.

[19] T. Tanabe, M. Kawasumi, and M. Yamashita, “Thermal Stress Analysis of Massive Concrete”, in *Seminar Proceedings For Finite Element Analysis of Reinforced Concrete Structures*. 1986.

[20] Midas Civil, “Analysis for Civil Structures”. [Online]. Available: https://www.midasbridge.com. [Accessed: 7 Jan. 2025].

[21] Y. Huang, G. Liu, S. Huang, R. Rao, and C. Hu, “Experimental and Finite Element Investigastion on The Temperature Field of a Massive Bridge Pier Caused by The Hydration Heat of Concrete”, *Construction and Building Materials*, vol. 192, pp. 240–252, 2018, doi: 10.1016/j.conbuildmat.2018.10.128.

[22] S. Tatro and E. Schrader, “Thermal Analysis for RCC-A Practical Approach”, in *ASCE Specialty Conference on Roller Compacted Concrete*. ASCE, 1992, pp. 389–406.

[23] Midas Civil Tutorial, Heat of Hydration Analysis by Construction Stages, 2024.

[24] Cement Concrete & Aggregates, “Part V Concreting Site Practices Hot and Cold Weather Concreting”, Australia, 2020. [Online]. Available: https://www.ccaa.com.au. [Accessed: 7 Jan. 2025].

[25] M.R.H. Dunstan, “Rolled Concrete for Dam – Laboratory Trial of High Fly Ash Content Concrete”, *CIRIA Technical Note*, 1981.

[26] W.S. Adaska, “Roller-Compacted Concrete (RCC)”, American Cement Association. [Online]. Available: https://www.cement.org/wp-content/uploads/2024/08/sn2975.pdf. [Accessed: 7 Jan 2025].

Received: 2024-11-29, Revised: 2025-01-21